Challenges and breakthroughs in alpha radiation detection, with a focus on the innovative RemoteAlpha project

I.R. Nikolényi , Z. Gémesi

(1) Institute of Mathematics and Basic Science, (2) Research teacher, MATE Hungarian University of Agriculture and Life Sciences
Páter K. u. 1., Gödöllő, H-2100 Hungary
E-mail: Nikolenyi.Istvan.Robert@uni-mate.hu

Practical and Experimental Learnaing Day on „Detection of Radiological and CBRN materials”

May 09, 2024, Gödöllő, Hungary

HUNGARIAN UNIVERSITY OF AGRICULTURE AND LIFE SCIENCES

Partners of EMPIR 2020 19ENV02 RemoteAlpha project.

Physikalisch-Technische Bundesanstalt

Budapest Főváros Kormányhivatala

"Horia Hulubei" National Institute for R&D in Physics and Nuclear Engineering

Alfa Rift Oy

Alfa Rift Oy

Tampereen korkeakoulusäätiö sr

Gottfried Wilhelm Leibniz Universität Hannover

Universitat Politècnica de Catalunya

Szent István University

This project 19ENV02 RemoteALPHA has received funding from the EMPIR programme co-financed by the Participating States and from the European Union's Horizon 2020 research and innovation programme.

Information about EMPIR 2020 19ENV02 RemoteAlpha project.

MAGYAR AGRÁR- ÉS ÉLETTUDOMÁNYI EGYETEM

https://www.euramet.org/researchinnovation/search-research-projects/details/project/remote-and-real-timeoptical-detection-of-alpha-emitting-radionuclides-in-the-environment/.

https://remotealpha.drmr.nipne.ro/partners.php

SEARCH | LOGIN | MENU

The gateway to Europe's integrated metrology community.

Home | Newsletter | Contact us | LinkedIN | YouTube | Twitter

EURAMET

ABOUT EURAMET | EUROPEAN METROLOGY NETWORKS | IMPACT, INNOVATION & RESEARCH PROGRAMMES | GUIDES & PUBLICATIONS | KNOWLEDGE TRANSFER & CAPACITY BUILDING | TECHNICAL COMMITTEES & TC PROJECTS

Research & Innovation | Search Research Projects

Remote and real-time optical detection of alpha-emitting radionuclides in the environment

Short Name: RemoteALPHA, Project Number: 19ENV02

Man in protective workwear

COORDINATOR
Fatou Krasniqi (PTB)

PARTICIPATING EURAMET NMIS AND DIS
- BFKH (Hungary)
- IFIN-HH (Romania)
- PTB (Germany)

OTHER PARTICIPANTS
Alfa Rift Oy (Finland)
Gottfried Wilhelm Leibniz Universität Hannover (Germany)
Magyar Agrár- és Élettudományi Egyetem (Hungary)
Tampereen korkeakoulusäätiö sr (Finland)
Universitat Politécnica de Catalunya (Spain)

INFORMATION

PROGRAMME
EMPIR

FIELD
Environment

STATUS
in progress

CALL
2019

DURATION
2020-2023

Remote and real-time optical detection of alpha-emitting radionuclides in the environment

Home | Project | Information | Members Area | Blog | Contact | GDPR

OTHER PARTICIPANTS

Alfa Rift Oy (Finland)
Gottfried Wilhelm Leibniz Universität Hannover (Germany)
Magyar Agrár- és Élettudományi Egyetem (Hungary)
Tampereen korkeakoulusäätiö sr (Finland)
Universitat Politécnica de Catalunya (Spain)

Need for novel-type detection system for alpha emitters

„…Due to the short range of alpha particles, traditional detectors which require direct interaction with the alpha particles must be used in very close proximity to a contaminated surface, around 1 cm…"

Crompton et al (2018), Sensors, 18, 1015; doi:10.3390/s18041015

- Attacks on nuclear power plants
- deployment of the dirty bomb (have a shocking effect on public opinion.)
- the poisoning of Litvinenko with the alpha emitting isotope 210-Po. He was an agent of the KGB and then the Federal Security Service. He died on 26th November 2006 , London.
- Previous serious reactor accidents (Chernobyl, Fukushima)

„…Alpha particles represent the biggest risk to soft biological tissues compared to all nuclear decay products due to their high energy, large mass and high linear energy transfer. The amount of deposited energy is about 2 000 000 to 6 000 000 times higher than that of an ordinary chemical reaction (ordinary chemical energy used by the cells in the body), thus implying that a single alpha particle has the ability to severely damage or kill all cells within its range (typically, two to four cells). Therefore, the release of alpha emitting radionuclides in the environment, such as by nuclear terroristic attacks or transportation accidents, as well as by severe emergencies in nuclear installations, represents the greatest radiological threat for human beings if they enter the human body…."

„…A detection system to measure large-scale contamination of these radionuclides is currently not available…"

(Publishable Summary for 19ENV02 RemoteAlpha)

ails and *results* of the project are in Publishable
mmary

MAGYAR AGRÁR- ÉS ÉLETTUDOMÁNYI EGYETEM

,…New instrumentation for the optical detection of alpha particle emitters in the environment…" (Newsletter: October, 202
This is a passive method

To develop and establish a calibration system for the novel-type radioluminescence detector systems.

To extend the optical detection system to an imaging functionality for mapping of alpha contaminations in the environme
ng tripod and unmanned aerial vehicle (UAV)

easibility study for an active, complementer method, namely laser-induced fluorescence (LIF) spectroscopic method for
detection of alpha emitters

https://www.euramet.org/research-innovation/search-research projects/details?tx_eurametctcp_project%5Bproject%5D=1687&cHash=c8e79ec377e929c4b2f6a63

•Publishable Summary Publishable Summary Remote and real-time optical detection of alpha-emitting radionuclides in the environment (19ENV02), Call 2019 0.22 MB

Alpha-radioluminescence phenomenon, its spectrum and measuring technique (Baschenko's results)

MAGYAR AGRÁR- ÉS ÉLETTUDOMÁNYI EGYETEM

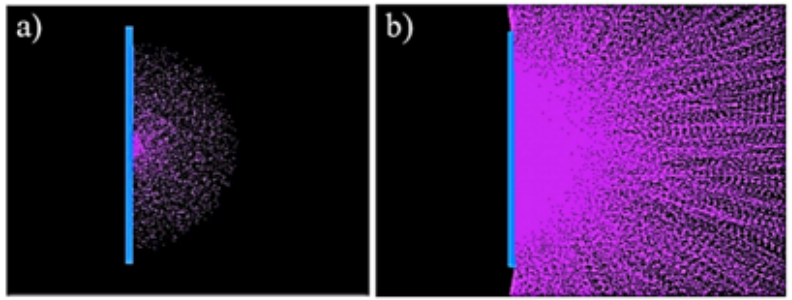

Figure 3. Model of: (a) Radioluminescence photons induced by alpha particles showing the hemisphere in which they are initially created by the alpha particles; (b) Showing the random directions in which the photons are emitted from the hemisphere in (a) and their longer path length—Using FRED Optical Engineering Software (Photon Engineering LLC) [11]. Reprinted with permission from the author.

sensors

MDPI

Review

Alpha Particle Detection Using Alpha-Induced Air Radioluminescence: A Review and Future Prospects for Preliminary Radiological Characterisation for Nuclear Facilities Decommissioning

Anita J. Crompton [1,*], Kelum A. A. Gamage [2], Alex Jenkins [3] and Charles James Taylor [1]

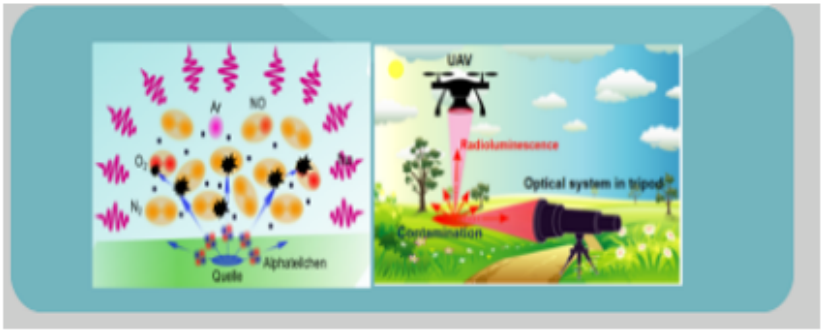

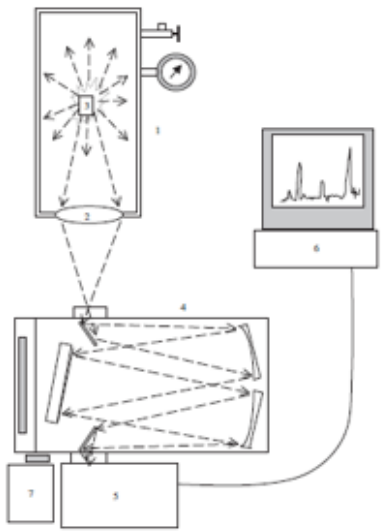

Figure 1. The scheme of the experimental set-up for the atmosphere alpha-radioluminescence phenomenon spectral investigation: 1—chamber diameter 400 × 1500 mm³; 2—window-lens diameter 200 mm, $F = 500$ mm; 3—alpha particle source; 4—monochromator; 5—photodetector; 6—PC; 7—stepping motor.

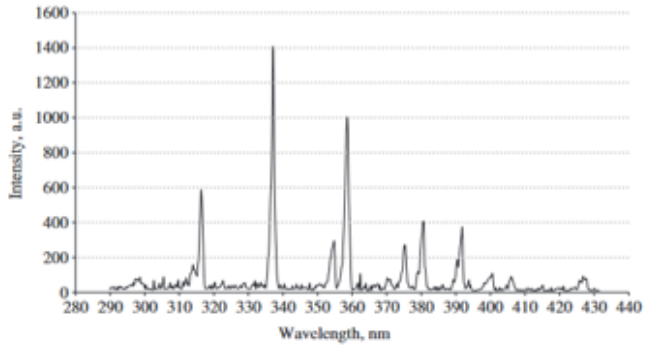

Figure 3. The optical spectrum of atmosphere alpha-radioluminescence under standard conditions.

The main emitter is molecular nitrogen (and also nitrogen ion)

The air is a poor scintillator. Oxygen and water vapour quenche the radioluminescence !!!

INSTITUTE OF PHYSICS PUBLISHING JOURNAL OF RADIOLOGICAL PROTECTION
J. Radiol. Prot. **24** (2004) 75–82 PII: S0952-4746(04)75622-0

Remote optical detection of alpha particle sources

Sergiy M Baschenko

Thomas Kerst's results (Academic Dissertation, 2017, Tampere University)

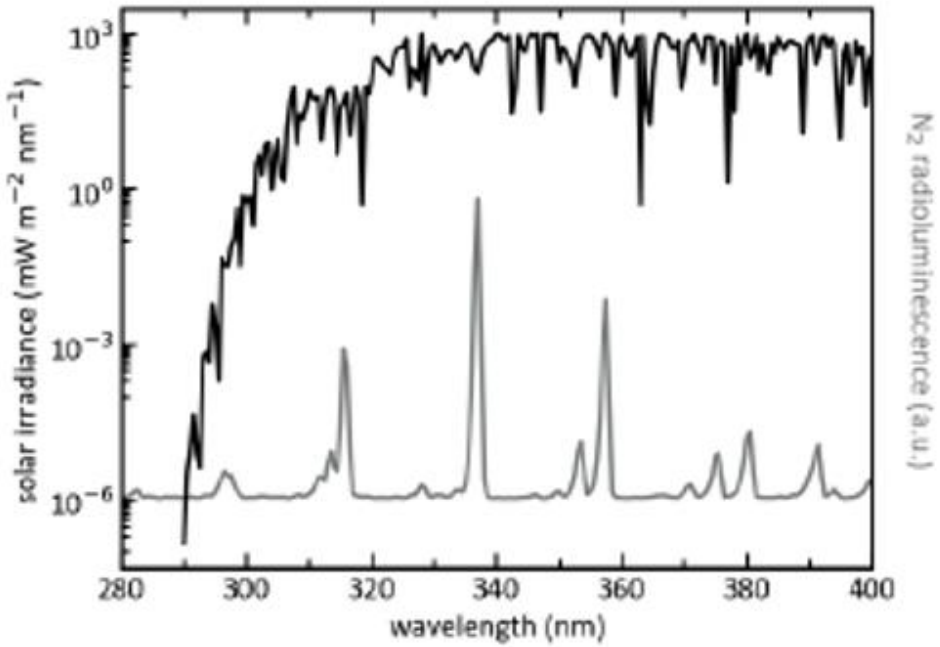

Fig. 1. Spectrum of sunlight reaching the earth's surface (black) contrasted with the radioluminescence of N_2 (gray) in the wavelength range 280 nm – 400 nm. The solar irradiance (AM1.5 Global tilt [11]) is displayed on a logarithmic scale, while the N_2 emissions are shown on a linear scale. At wavelengths longer than 290 nm the solar irradiance spectrally overlaps with the radioluminescence of N_2.

„…Excitation of NO by excitation transfer via interaction with N2 molecules appears to be able to explain our data. In this process, molecular nitrogen in the long-lived N2 state excites ground state nitric oxide to the NO state, while the N2 molecule loses its excitation and decays to the ground state…"

Research Article | Vol. 26, No. 26 | 24 Dec 2018 | OPTICS EXPRESS 33770
Optics EXPRESS

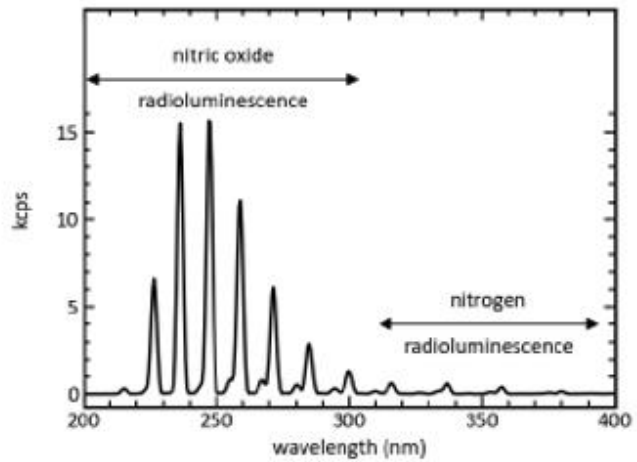

Fig. 4. Radioluminescence spectrum of gas a gas mixture containing 50 ppm of NO diluted in N_2. The nitric oxide emission is about 25 times stronger than N_2 emission and most of the NO emission lines are located in the solar blind spectral region.

Table 1. The intensity of radioluminescence between 200 nm – 400 nm for three different gas environments. The intensity is expressed in relation to the intensity found in normal air, highlighting the improvement in photon yield by changing gases. The energy conversion efficiency shows how much of the energy deposited in air by an alpha particle is emitted as light.

Gas environment	Radioluminescence intensity	Energy conversion Efficiency	Reference

Demonstration of an order-of-magnitude enhancement of scintillation using a gas mixture of N2 +NO in UV-C solar blind range

MAGYAR AGRÁR- ÉS ÉLETTUDOMÁNYI EGYETEM

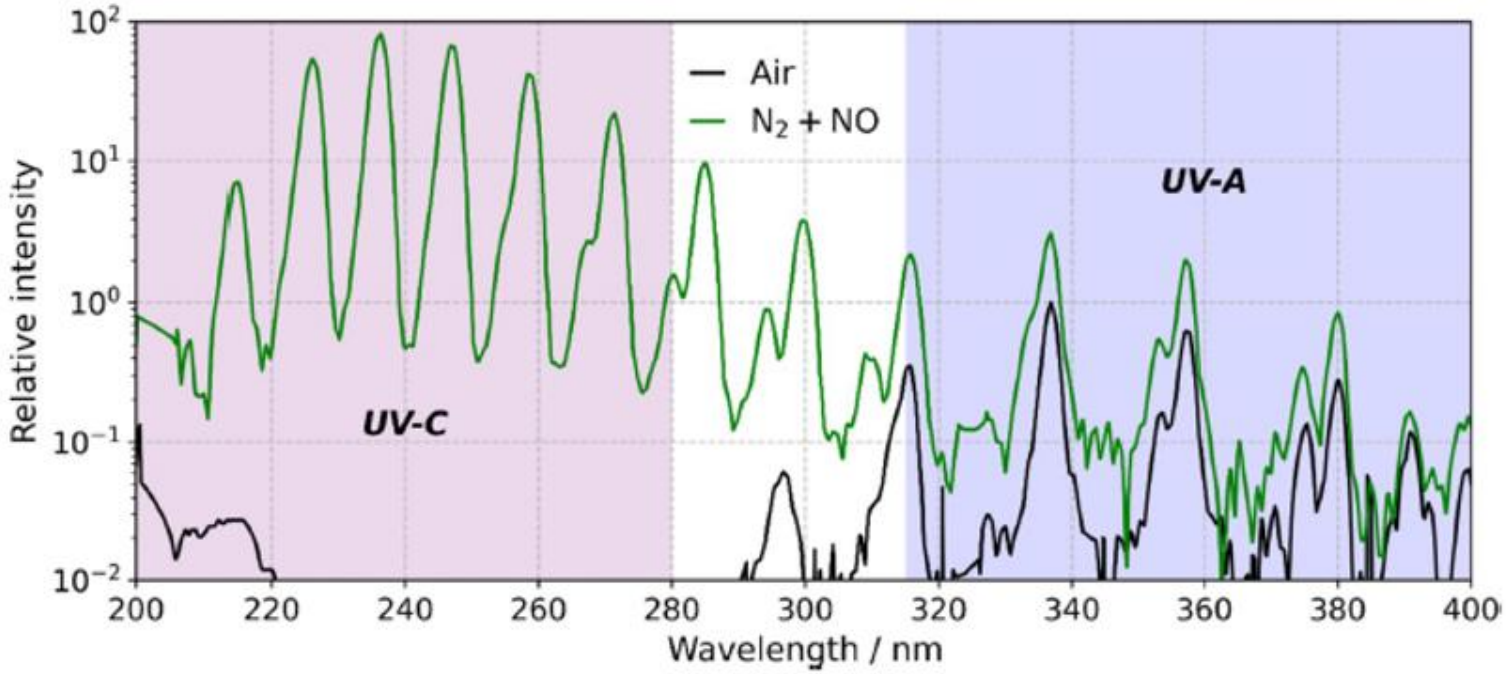

Journal of Radioanalytical and Nuclear Chemistry
https://doi.org/10.1007/s10967-023-09235-2

Radioluminescence mapping of ^{241}Am-doped environmental sampl and nuclear materials

Maksym Luchkov[1] · Claudia Olaru[2] · Ioana Lalau[2,4] · Mastaneh Zadehrafi[2] · István Róbert Nikolényi[3] Zoltán Gémesi[3] · Mihail-Razvan Ioan[2] · Faton Krasniqi[1]

Received: 31 July 2023 / Accepted: 22 October 2023

Fig. 1 Typical alpha radioluminescence spectrum measured in dry air at normal temperature and pressure (NTP) and N_2+NO gas atmosphere with 2 ppm NO. In air, more than 95% of the total intensity is contained in the UV-A and UV-B spectral region (within 310 nm to 400 nm), while the intensity of UV-C radioluminescence (below 280 nm) is very low (<5%). The radioluminescence signal in the UV-C spectral region can be enhanced by more than three orders of magnitude by purging the space around the alpha source with N_2+NO gas mixture. The spectra are measured with a CAS140D spectroradiometer at the PTB Ion Acceleration Facility (PIAF) with a narrowly collimated beam of 5 MeV alpha particles. The intensities are normalized to the 337 nm spectral line of air radioluminescence

The first laboratory CCD camera-based results on UV-C imaging and scannings

Krasniqi et al , 2021: Nuclear Inst. and Methods in Physics Research, A 987 (2021) 164821

- (a wide field-of-view (FOV) imaging system in conjunction with an intensified CCD camera (hereafter, CCD-based imaging system)

.

- a narrow FOV Galilean-type telescope combined with a cesium-telluride photocathode photomultiplier (hereafter, scanning PMT system).

The distance between the detection system and the sample was between 0.4 to 0.53 meter.

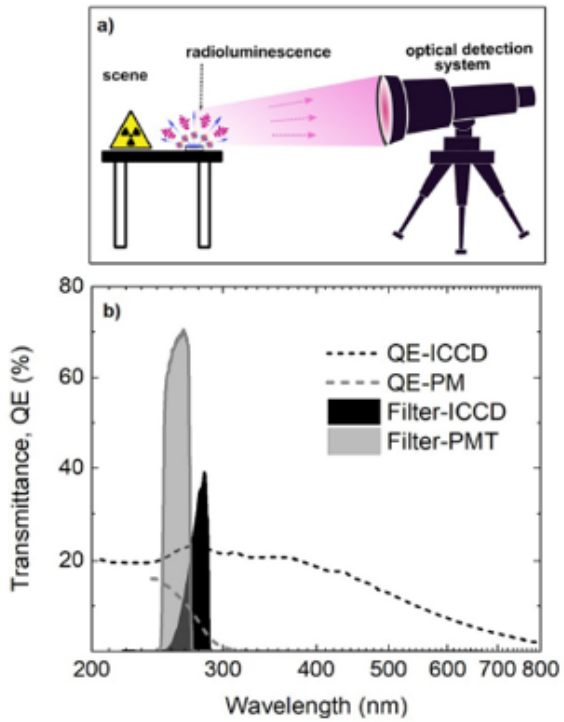

Fig. 1. (color online) (a) Schematic of the UV-C imaging setup. Radioactive material is placed either on the table or inside a steel chamber. The detection system is placed between 0.4 to 0.53 m away from the sample. (b) Quantum efficiency curves of the used detectors (ICCD camera and cesium-telluride photocathode photomultiplier tube) and transmission of the UV-C filters.

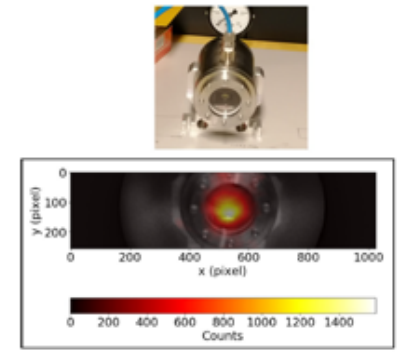

Fig. 3. (color online) UV-C radioluminescence imaging of 3.7 MBq source (lower panel) and a photograph of the sample in the experimental chamber (upper part). The alpha source was placed on a steel chamber with a quartz window, flushed with N_2 (6.0 purity) at a rate of 5 L/min. The NO concentration was 50 ppb.

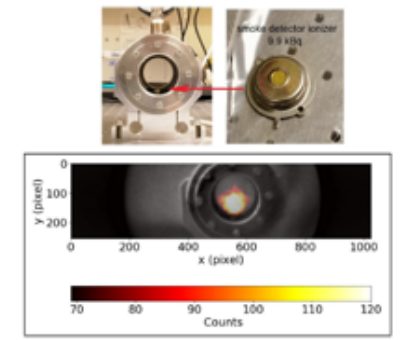

Fig. 4. (color online) UV-C radioluminescence image of a 9.9 kBq smoke detector ionizer. The concentration of NO at the N_2 atmosphere was about 3 ppm.

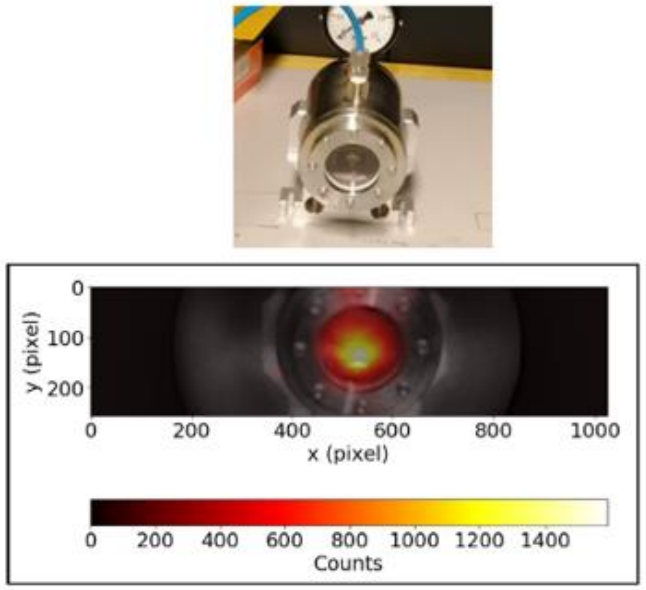

Fig. 3. (color online) UV-C radioluminescence imaging of 3.7 MBq source (lower panel) and a photograph of the sample in the experimental chamber (upper part). The alpha source was placed on a steel chamber with a quartz window, flushed with N_2 (6.0 purity) at a rate of 5 L/min. The NO concentration was 50 ppb.

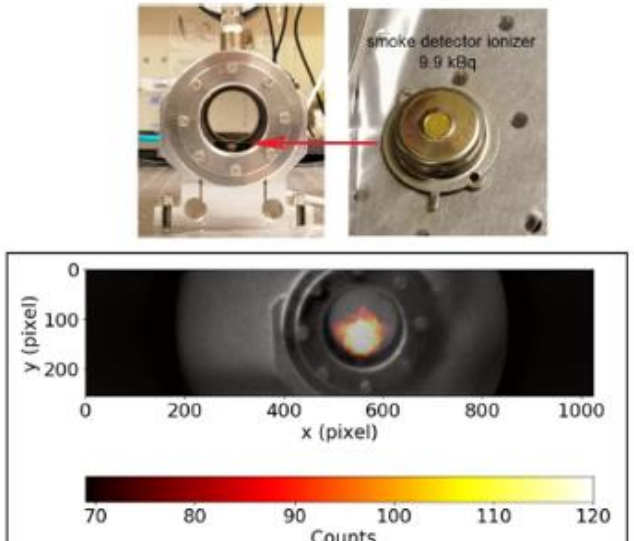

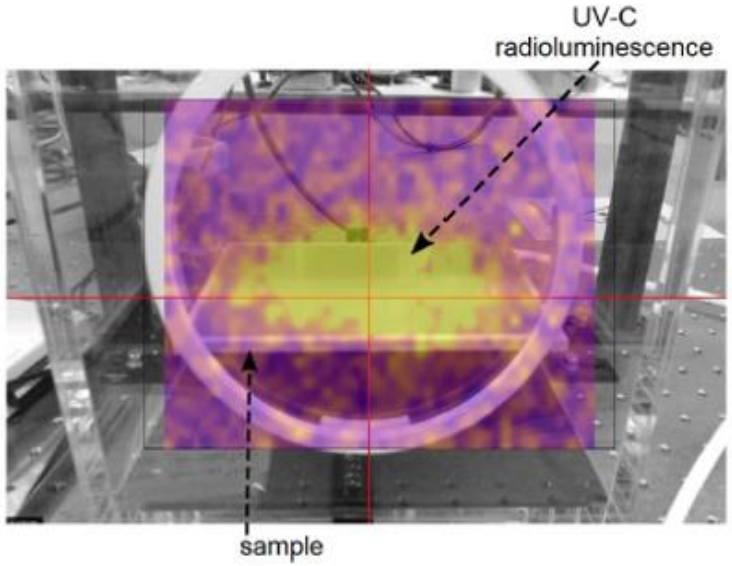

ig. 6. (color online) Image of a wide area reference alpha-emitting source composed of the uranium isotopes U-234, U-235 and U-238, with a total activity of 330 Bq over n active area of 19.1 × 11.9 cm². The concentration of NO at the N_2 atmosphere vas about 3 ppm. The scene was scanned using scanning PMT system at about 0.4 m listance with a resolution of 1 deg and 30 s integration per point.

an average signal level of about 75 cps and a noise level of about 31 cps. To the best of our knowledge, this is the lowest activity imaged using UV-C radioluminescence to date. The present results indicate that optimizing such imaging techniques can push the detection limit even further down and such techniques might also be used for determination of legal limits in the future.

„…the feasibility of detecting low activity in environmental samples by measuring their radioluminescence with the optical detection system …"

A. Klose et al 2022: Journal of Radioanalytical and Nuclear Chemistry (2022) 331:5401–5410

Sample	Origin	Size [cm²]	Mass [g]	Picture
J	Wölsendorf	13.1	16.4	
K	Wölsendorf	14.5	38.61	
L	Puy de Dôme	6.6	5.69	

- As calibration standard, pitchblende minerals were prepared
- alpha-track-detection was used for analysing the homogeneity of the alpha-emitter distribution on the pitchblende samples
- alpha-spectroscopy was performed using a grid ionisation chamber (GIC). with *P10*, a gas mixture of 90% argon and 10% methane, at a pressure of 1.025 bar.

Preparation

Pitchblende bearing ores from different locations with a comparatively high uranium content were cut into 5 mm thick slices with a micro-waterjet. The resulting surface is flat but not polished. The shape of the samples is irregu-

Fig. 3 Alpha-track of sample L after 1 min exposure
Raw data shown in (a). Adjusting the threshold generates a black-white-image (b). The tracks are highlighted and can be further analysed. For this example, the number of tracks was counted. It is 548 on a total area of 2.49 mm by 1.87 mm.

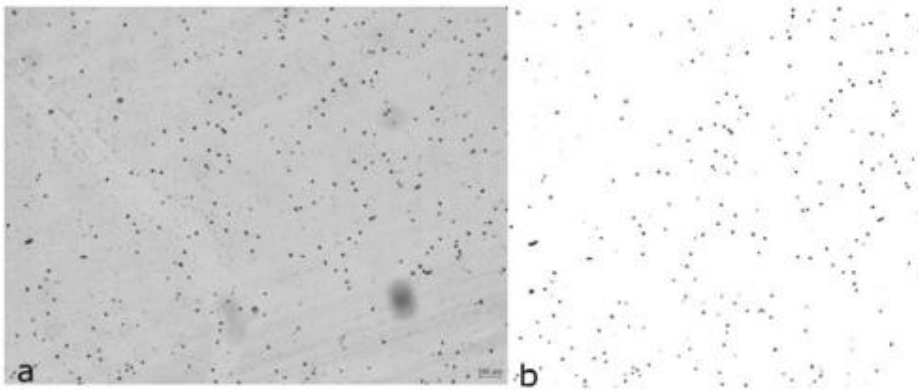

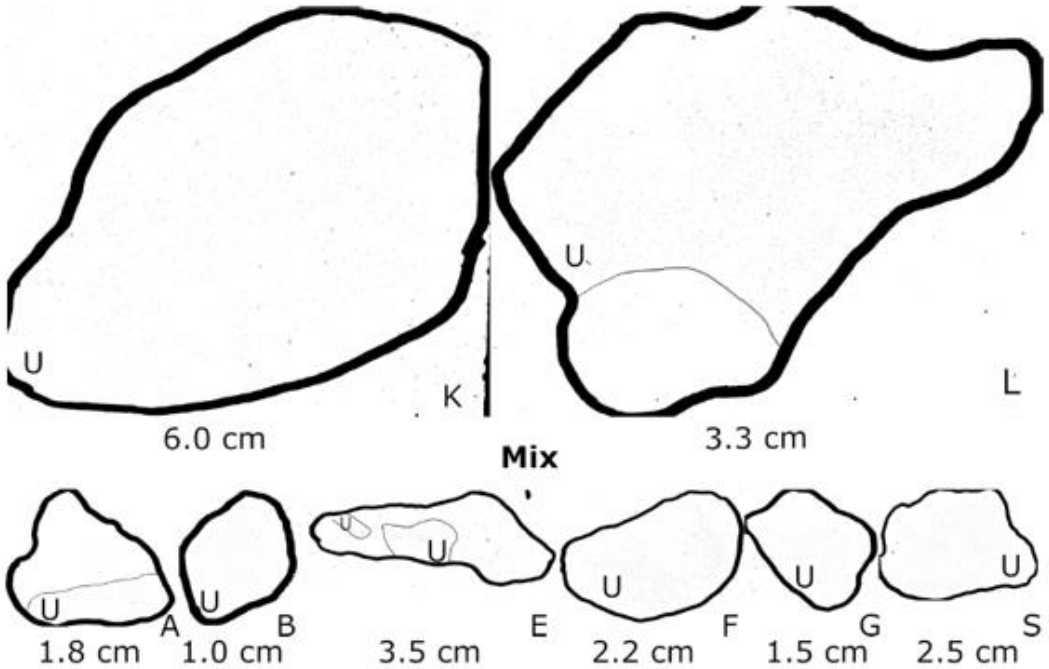

Fig. 4 Alpha-Track-Images of three different samples
Except for A and E from sample Mix, the alpha-emitters are homogeneously distributed over the entire surface area. Areas containing much uranium and its daughters are labelled with "U"

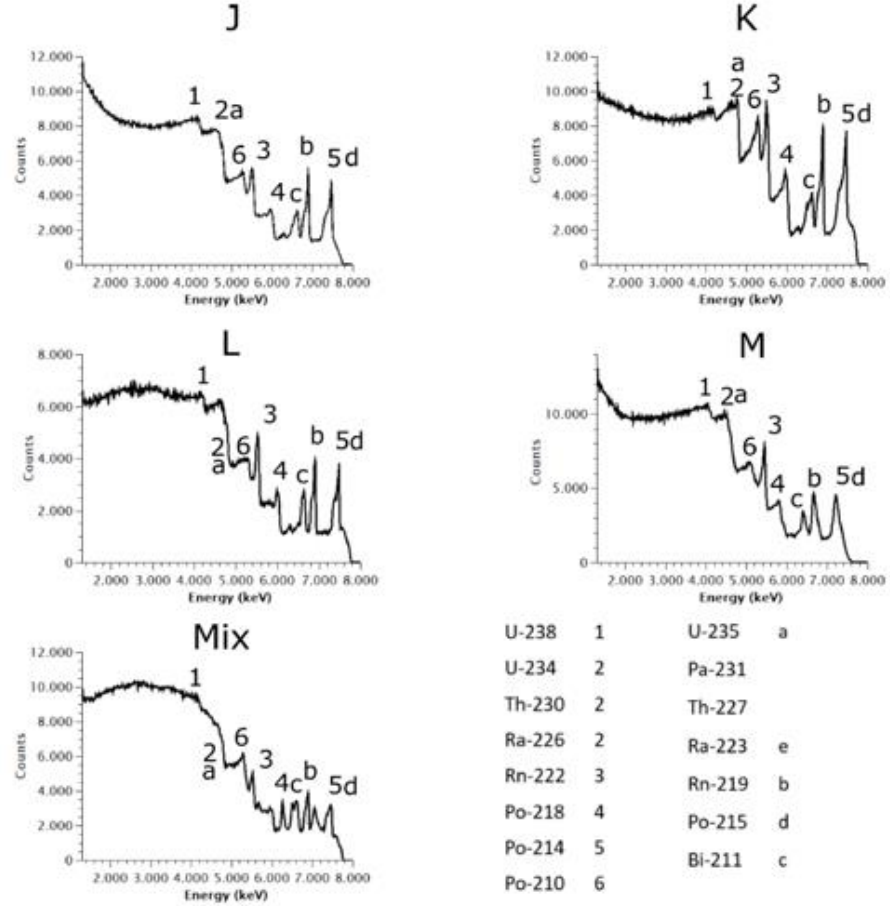

Fig. 5 GIC-Spectra of pitchblende samples J, K, L, M and Mix
The measurement time was normalized to 3000 s for each spectrum. They show a large amount of low energy alpha particles due to self-absorption. Numbers identify nuclides of the ^{238}U decay chain whereas letters identify nuclides of the ^{235}U decay chain

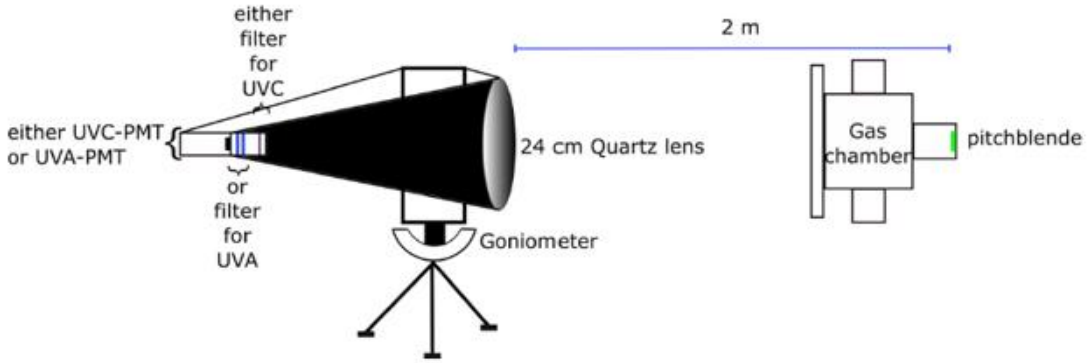

Fig. 1 The optical scanning system
The optical system is mounted at a distance of 2 m away from the sample. Depending on the kind of measurement, the gas chamber can be filled with air or different gas mixtures like N_2 and 10 ppm NO. The PMT and corresponding set of filters is changed for measurements in UVA and or UVC

Fig. 7 Arrangement of different pitchblende samples and UVA-Scan in air for 64 h

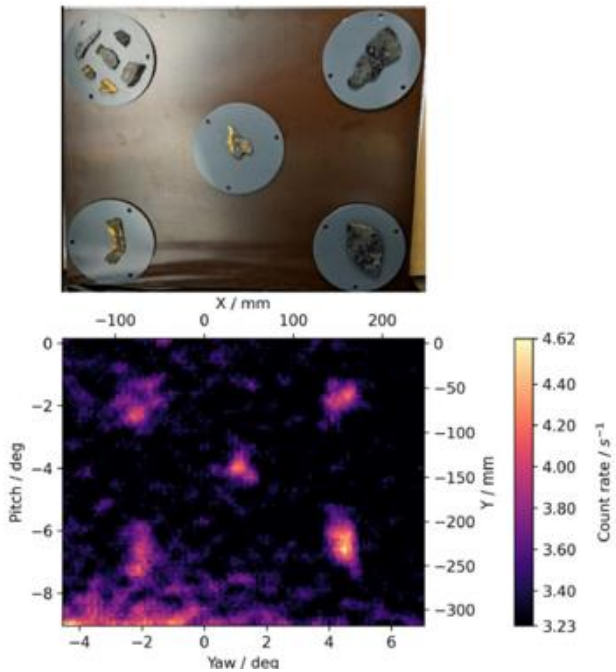

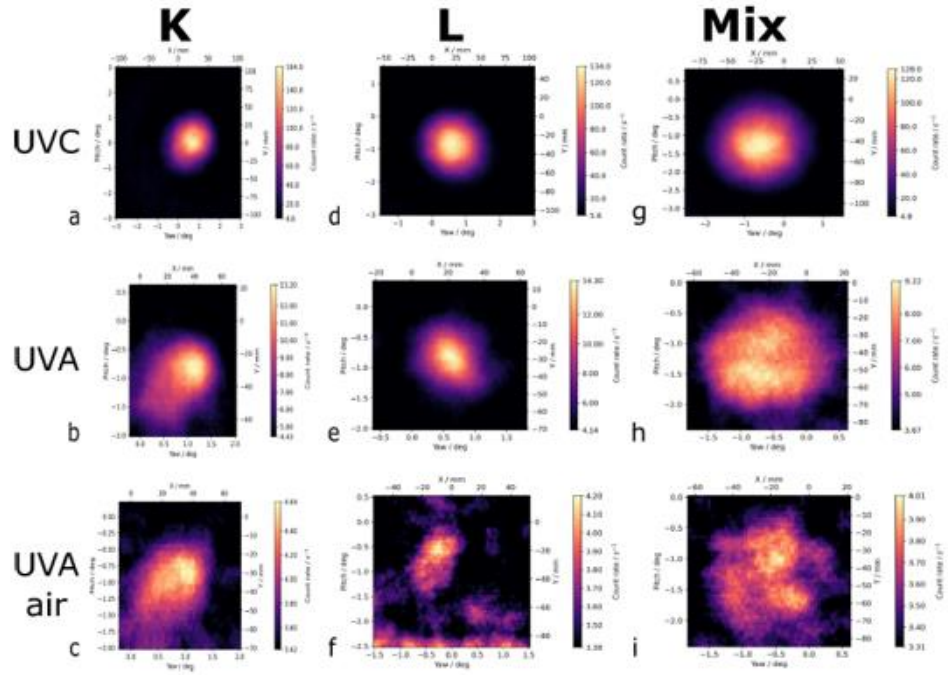

Fig. 6 Radioluminescence scans
The measurement in UVC yields the highest intensity for all samples (upper row) and the biggest radioluminescence glow. Both measurements in UVA have a smaller glow due to the smaller field of view. The background rate is higher as for measurements in UVC. Using the artificial atmosphere (middle row) leads to a three times higher signal than measuring in air (lower row). All samples have a similar surface activity and a similar photon count rate.

Table 5 Comparison of surface alpha count rate with photon count rates of the radioluminescence measurements

Sample	GIC (CPS)	UVC (CPS)	UVA (CPS)	UVA air (CPS)
K	1520(39)	1E6	3E3	6E1
L	1023(32)	2E5	3E3	1E2
Mix	1493(39)	4E5	4E3	5E1

The two optical ranges and the developed lens-filter-PMT based measuring systems, M.Luchkov et al, 2022: Nuclear Inst. and Methods in Phys. Research, A

MAGYAR AGRÁR- ÉS ÉLETTUDOMÁNYI EGYETEM

For all measurements in the UV-C spectral region, the Hamamatsu PMT with CsTe photocathode (H11870-09) was used with bandpass interference filters having a bandwidth of 16 nm and center wavelength of 260 nm (FF01-260/16–25, Semrock Inc.).

In the UV-A spectral range, Hamamatsu PMT with ultra-bialkali photocathode (H10682-210) was used with interference filters centered at 337 nm with a bandwidth of 10 nm (# 65–128, Edmund Optics). Both PMTs were selected for a very low dark rate, i.e. the UV-C PMT has a dark count rate of less than $1\ s^{-1}$, while the UV-A has less than $10\ s^{-1}$.

- high-quality UV fused silica (UVFS) lens, for tripod

.and the other two were

- PMMA (Poly(methyl 2methylpropenoate) Fresnel lenses for UAV

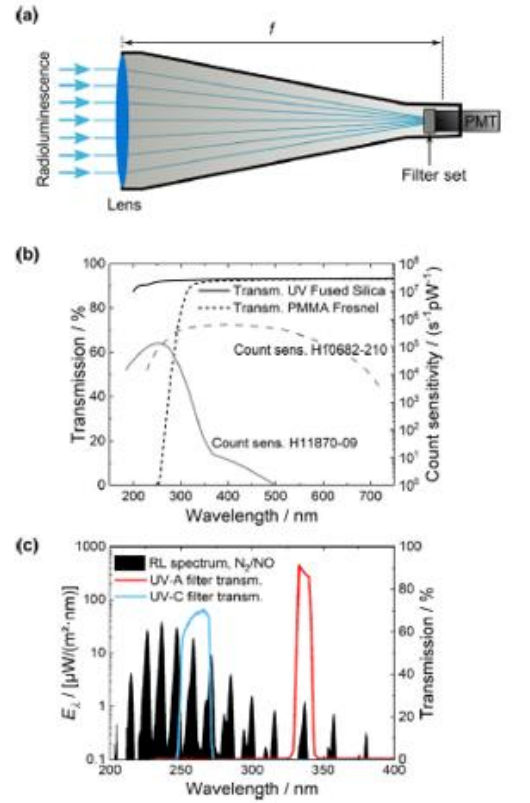

Fig. 2. (a) Schematic drawing of optical systems developed in the framework RemoteALPHA project. Both, the UVFS- and PMMA Fresnel-lens systems share t same configuration: they utilize large receiving optics to maximize the geometri factor, and the focal lengths have been chosen such that the radioluminescence ima is not blurred substantially by the overlapping FOVs between adjacent scanning poin (b) Transmittance spectra of UVFS [22] and PMMA [23] together with the PM count sensitivity [24,25] specified by the manufacturer. (c) Radioluminescence emissi spectrum of NO measured at the PIAF at a nominal alpha particle rate of abc $30 \times 10^6\ s^{-1}$ with a PTB-calibrated array spectroradiometer with UV-C and UV-A fil transmission [26,27]. The flow rate of N_2+NO was set at 2400 mL·min^{-1} with N concentration of 5 μL·L^{-1}.

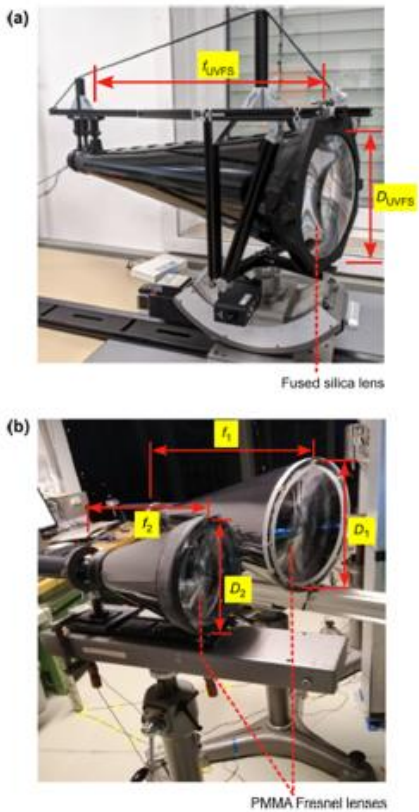

Fig. 3. Lens-based radioluminescence detection setups. (a) Fused silica lens (Abet Technologies) system mounted on a goniometer and rotation stage (Newport M-BGM160PE and RVS80CC) with D_{UVFS} = 240 mm and f_{UVFS} between 572 mm to 599 mm in a wavelength range from 236 nm to 285 nm, respectively. (b) PMMA Fresnel lens systems with lenses (Orafol Fresnel Optics) having diameters D_1 = 452.9 mm (SC 2045) and D_2 = 257.6 mm (SC 210), and nominal focal lengths f_1 = 391.5 mm and f_2 = 225.5 mm at 546 nm. All lens systems can be coupled to Hamamatsu PMTs (H10682-210 for UV-A spectral range and H11870-09 for UV-C spectral range) and UV-C filters (FF01-260/16-25, Semrock Inc.) or UV-A filters (337 nm, 10 nm band-pass filters from Edmund Optics).

Test and demonstration of the radioluminescence mapping capability

The radioluminescence mapping capability is demonstrated with the UVFS telescope which has been used to obtain the radioluminescence image of (a) deceleration of alpha particles at the exit port of the PIAF microbeam, (b) dedicated Am-241 sample designed to simulate an extended alpha source, and (c) low activity pitchblende minerals with surface activity between 80 $Bq\,cm^{-2}$ and 105 $Bq\,cm^{-2}$.

- The detection efficiency of all systems

has been measured at the PTB Ion Accelerator Facility (PIAF) where alpha particles with a rate from 5×10^4 s^{-1} to about 4.5×10^7 s^{-1}, collimated to a beam size of 100 µm × 100 µm, have been accelerated to energies up to 8.3MeV.

- The relationship between radioluminescence

photons and alpha activity is calibrated with a dedicated 210-Po activity

Nuclear Inst. and Methods in Physics Research, A 1047 (2023) 167895

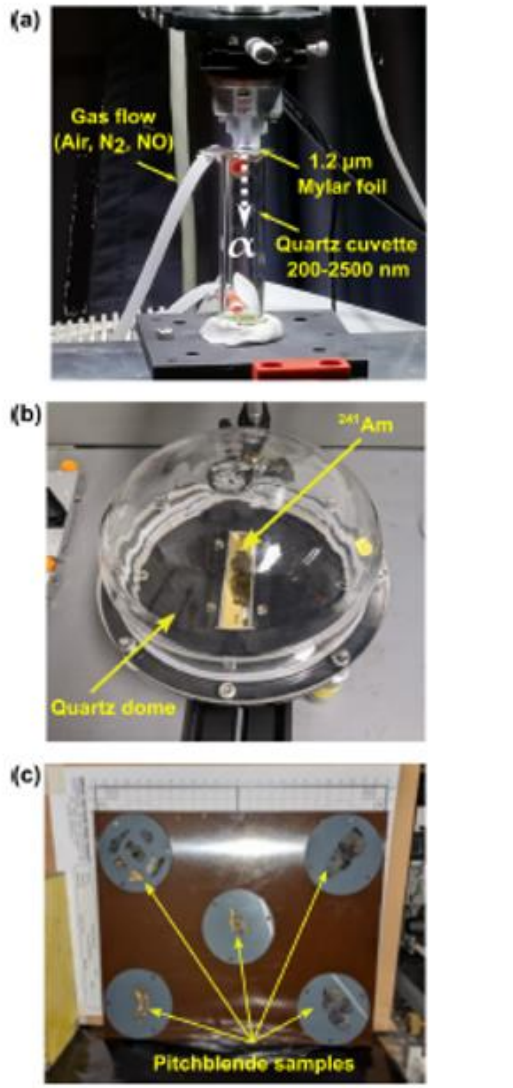

Fig. 4. (a) Photo of the alpha particle interaction region at the PIAF. The PIAF microbeam was focused into a quartz cuvette (Hellma Analytics, cylindrical quartz cuvette with two tubes, wavelength range 200 nm–2500 nm, 100 mm path length) which could be filled with different gases (air, N_2, N_2+NO mixture). (b) Photograph of the Am-241 source (Eckert & Ziegler Gario) inside a quartz dome. (c) Arrangement of pitchblende mineral samples. The samples were cut from pitchblende-bearing ores with a micro water jet into slices with flat unpolished surfaces (for details, see [29]).

In all cases, the radioluminescence count rate is linearly proportional to the alpha particle rate. At a reference distance of 2 m between the radioluminescence source (i.e., the cuvette in which the alpha particles are stopped) and the receiving optics, both lens systems capture a part of the alpha particle path length around the Bragg peak (i.e., the last 3 cm of their path). Since the energy loss curves around the Bragg peak are similar for energies between 5 MeV and 8.3 MeV used in these experiments, the sensitivity of both systems is relatively independent of the alpha particle energy. This observation can be seen in Fig. 6, where the radioluminescence count rates measured with

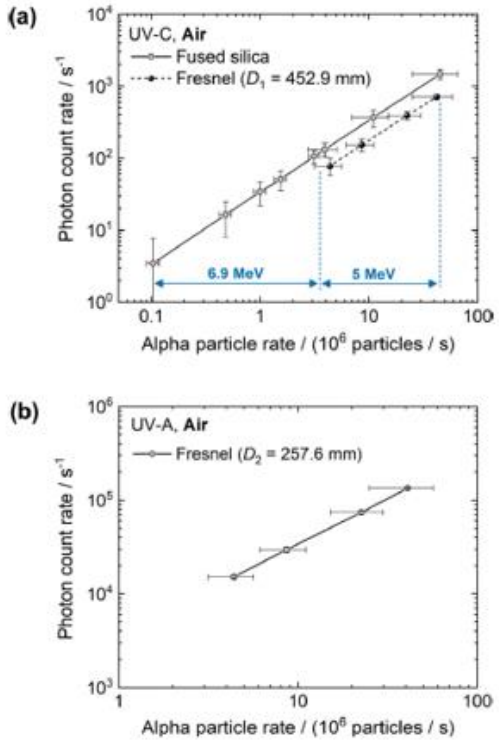

Fig. 6. (a) Comparison of UV-C radioluminescence sensitivities in air measured at the PIAF at a reference distance of 2 m between the radioluminescence source and lens. The slopes of linear fits are 34(6) s^{-1} MBq^{-1} for the UVFS and 17(3) s^{-1} MBq^{-1} for the Fresnel 1 (D_1 = 452.9 mm) lens systems at a background rate of 0.7(27) s^{-1} MBq^{-1} for both systems. Due to the finite FOV of both systems, the sensitivities for alpha particle energies of 5 MeV and 6.9 MeV are similar. (b) UV-A radioluminescence count rate generated by 5 MeV, measured with the Fresnel 2 lens system (D_2 = 257.6 mm). The signal slope is 3400(500) s^{-1} MBq^{-1}.

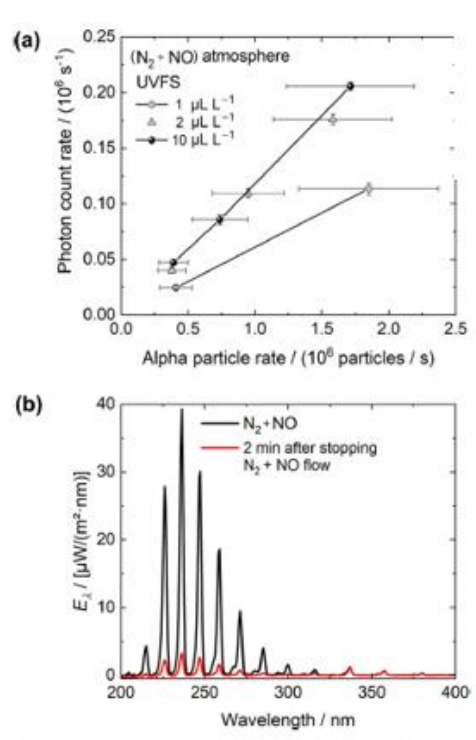

Fig. 7. (a) UV-C radioluminescence count rate generated by 5 MeV alpha particles, measured at the PIAF at a reference distance of 2 m between the radioluminescence source and the UVFS lens. The UV-C counting rate can be increased by more than three orders of magnitude by purging the cuvette with a N_2+NO gas mixture at a NO concentration above 2 µL L^{-1}. The UV-C sensitivity at 2 µL L^{-1} is 1.3×10^5 s^{-1} MBq^{-1}. At NO concentrations above 2 µL L^{-1}, the UV-C signal saturates. A similar trend is observed also with the Fresnel lens system. (b) Radioluminescence emission spectrum of NO measured at the PIAF at a nominal alpha particle rate of about 30×10^6 s^{-1} with a PTB-calibrated array spectroradiometer. Two minutes after stopping the flow of NO and N_2, the UV-C radioluminescence signal drops by a factor of 10 relative to the one measured with N_2+NO purging.

Table 1
Comparison between calculated sensitivities using Eq. (1) and those measured with the three lens-based radioluminescence detection systems.

Detection system	Lens material	Filters	PMT	Calculated sensitivity (s^{-1} MBq^{-1})	Measured sensitivity (s^{-1} MBq^{-1})
UVFS in UV-C	UV fused silica	2 filters (FF01-260/16–25, Semrock Inc.)	Hamamtsu H11870-09	36	34 ± 6
UVFS in UV-A	UV fused silica	2 filters (65–128, Edmund Optics)	Hamamtsu H10682-210	3810	Not measured
Fresnel 1 in UV-C	PMMA	2 filters (FF01-260/16–25, Semrock Inc.)	Hamamtsu H11870-09	18	17 ± 3
Fresnel 2 in UV-A	PMMA	2 filters (65–128, Edmund Optics)	Hamamtsu H10682-210	4500	3400 ± 500

$$s = \frac{\Omega}{4\pi} \cdot \int Y(\lambda) \cdot T_{\mathrm{src}}(\lambda) \cdot T_{\mathrm{lens}}(\lambda) \cdot T_{\mathrm{filt}}(\lambda) \cdot QE(\lambda) \cdot d\lambda \qquad (1)$$

where Ω is the solid angle in steradians, $Y(\lambda)$ photon yield expressed in photons per alpha particle [5], $T_{\mathrm{src}}(\lambda)$ is the transmission of the source enclosure (quartz cuvette for the beam), $T_{\mathrm{lens}}(\lambda)$ is the lens transmission, $T_{\mathrm{filt}}(\lambda)$ is the filter assembly transmission, and $QE(\lambda)$ is the quantum efficiency of the PMT in counts per photon. Filter transmission and quantum efficiencies of PMTs can be found on the

Steps of the calibration procedure of the radioluminecence detectors: determination of the sensitivity of the measuring system (240 mm UV fused silica lens-based) with standard 210-Po and 239-Pu alpha sources

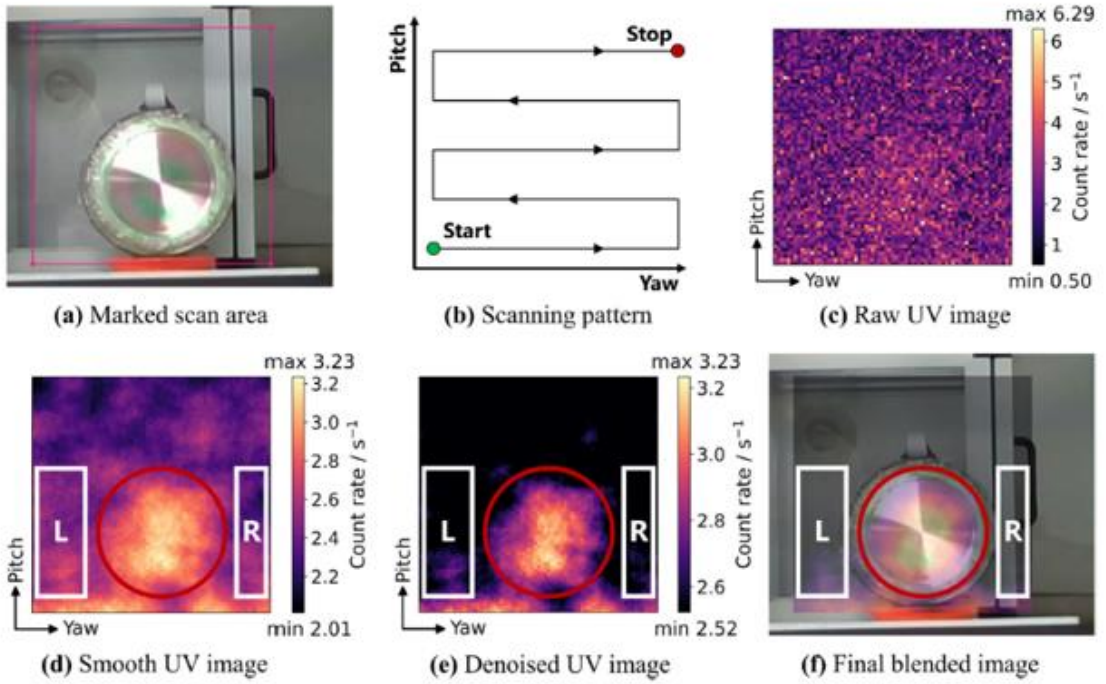

(a) Marked scan area (b) Scanning pattern (c) Raw UV image

(d) Smooth UV image (e) Denoised UV image (f) Final blended image

Fig. 4 The radioluminescence mapping procedure of the 4.9 kBq ^{239}Pu source measured in air from a distance of 2 m. The depth camera RGBD image **a** is used to select the scanning extent in pitch and yaw axes. The raw UV image **c** is smoothed using an averaging filter with a kernel size of 11 pixels. The smooth image **d** is then used to establish the signal and background domains: the source is outlined in red, and the background area (white) is selected according to the scan pattern **b** of the detector. The smooth data is further denoised through thresholding determined by the background signal, and the processed image **e** is superimposed onto the color image **a** to produce the final radioluminescence image **f**

Table 2 Sensitivity coefficients for the used radioluminescence imaging system configurations derived with reference sources of ^{210}Po and ^{239}Pu

Detector configuration	Sensitivity ($s^{-1}MBq^{-1}$)	
	^{210}Po (vacuum chamber)	^{239}Pu (airtight chamber)
UV-A, air	660 ± 80	760 ± 100
UV-C, N_2 + NO (saturated)	123,000 ± 14,000	63,000 ± 7000

The sensitivities are specified for a distance of 2 m between the source and the detector (lens)

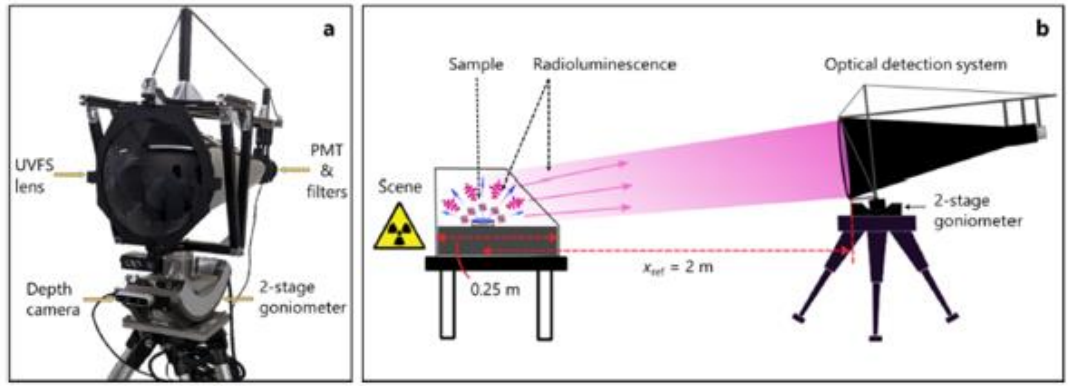

Fig. 2 **a** Radioluminescence imaging system built around a 240 mm diameter lens telescope. The system is mounted on a two-stage goniometer (Newport MBGM160PE and RVS80CC) and has an Intel RealSense D435 depth camera that captures an RGB color image of the scene. **b** Schematic diagram of radioluminescence mapping. The samples placed in the airtight enclosure are scanned by the optical system located 2 m away from the sample. The 2D image of the scene is obtained by scanning the optical system with the two-stage goniometer in pitch and yaw directions

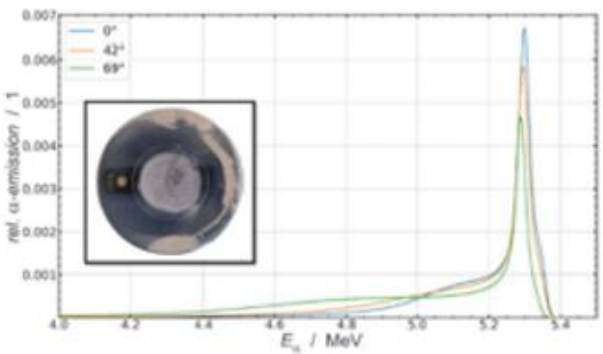

Fig. 3 *Relative alpha emission of ^{210}Po activity standard measured with a 25 mm² silicon surfac barrier detector behind a 3.2 mm aperture and a distance from the source surface of 15 mm. The spectra have been measured at 0°, 42° and 69° relative to the surface normal. The inset shows t ^{210}Po sample with a diameter of 12 mm (central part) deposited on the silver substrate.*

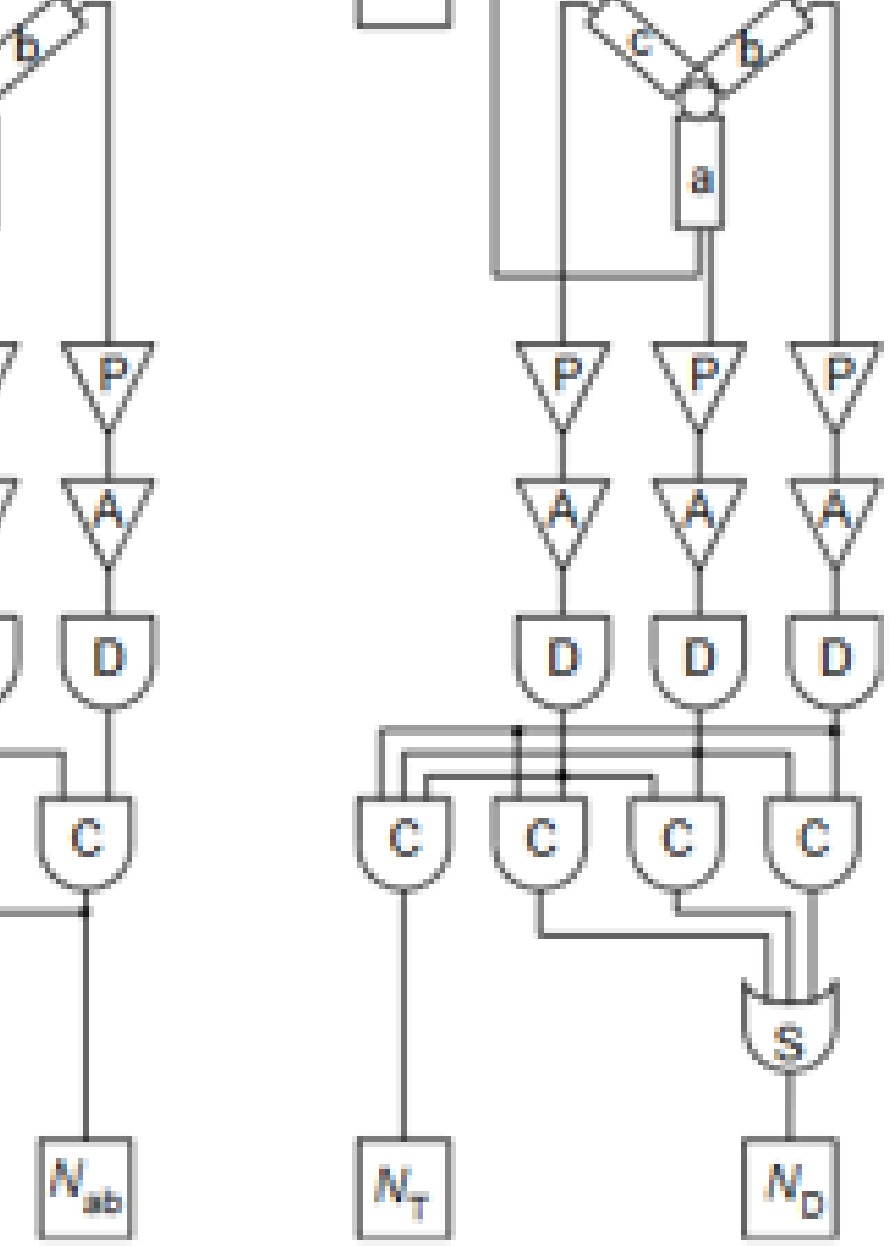

d block-diagram of the TDCR system with
or. (a) Schwerdtel's device, (b) Pochwalski's
voltage, P—preamplifier, A—amplifier, D—

differences from Schwerdtel's system. The
tally determined TDCR parameter, denoted

$$K = N_T/N_D$$

will always fall within an interval $0 \leqslant K \leqslant$
triple coincidence-counting rate, N_T, is a
than the double coincidence-counting rate,

As the counting efficiency approaches un

$$\varphi \to 1,$$

the double- and triple- coincidence-countin
approach the disintegration rate of the sou

$$N_T \to N_0,$$

$$N_D \to N_0$$

and the ratio K will also approach unity

$$K \to 1.$$

By extrapolating to $K = 1$, the values
tegration rate, N_0, with counting efficiency

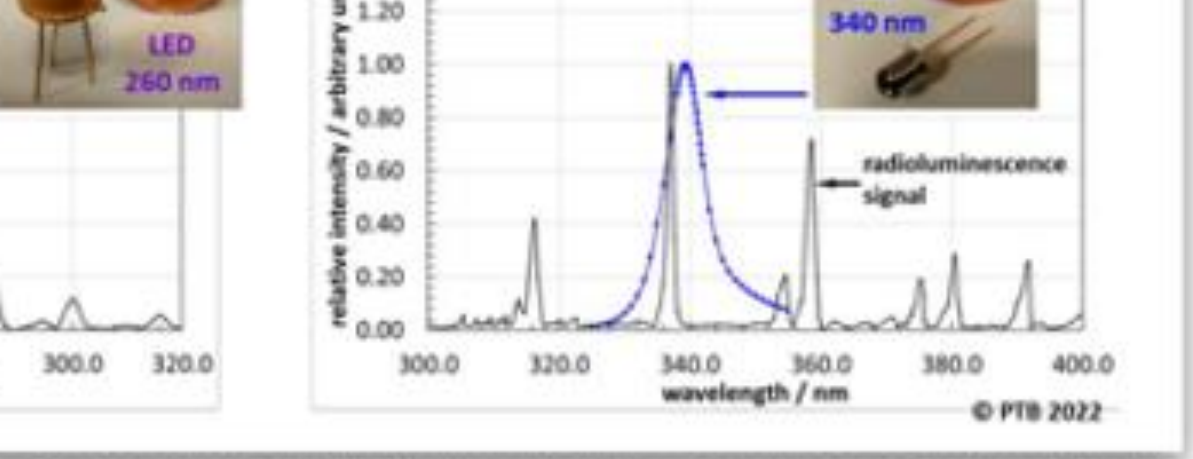

n in the ultraviolet (UV) wavelength spectral range induced in the air by alpha-particles
LED radiation sources.

radiance standard

and

from $2.9 \cdot 10^5$ Bq t
UV-C

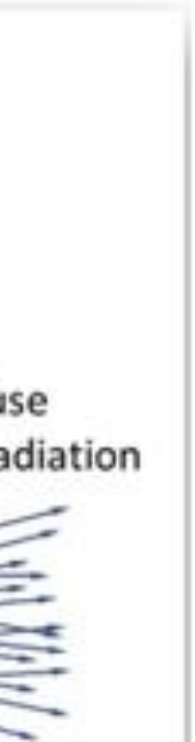

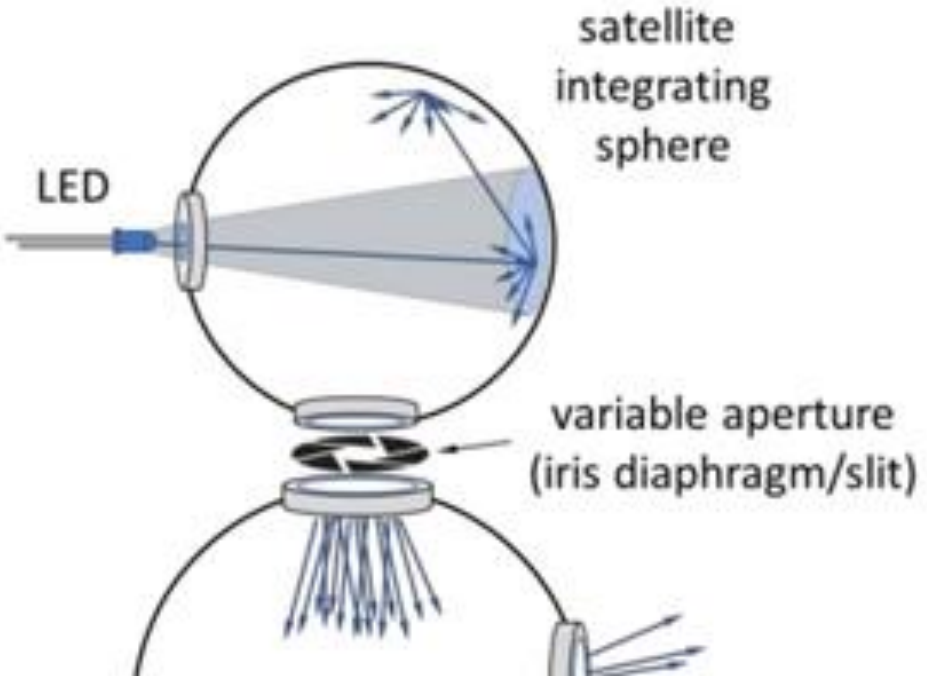

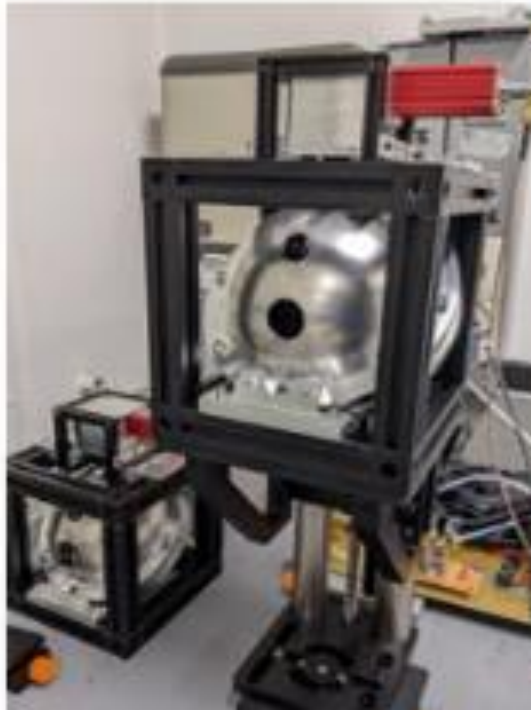

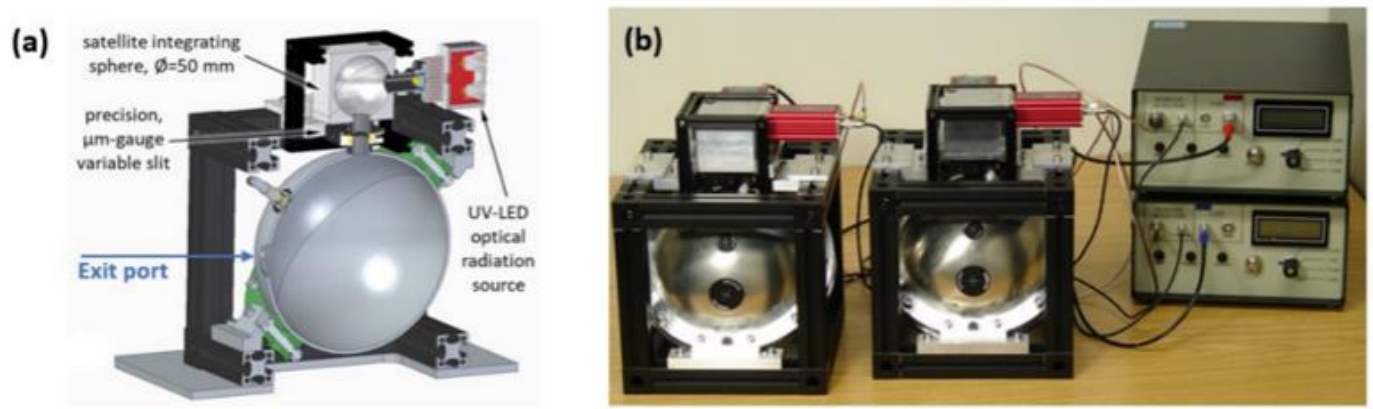

Figure 2: **(a)** Sectional schematic representation of the variable radiance, satellite integrating sphere-based configuration of the low photon flux UV radiance standard. **(b)** Realized prototypes of the variable low-photon flux UV-C (260 nm; left) and UV-A (340 nm; right) spectral range radiance standards for the calibration of the radioluminescence detector systems.

https://oar.ptb.de/resources/show/10.7795/EMPIR.19ENV02.PA.20231027

Krasniqi et al: A calibration methodology for the novel radioluminescence detector systems

el Carrera, J.; Rabago, D.; Duch,
Krasniqi, F. Mapping of Alpha-
ng an Unmanned Aircraft System.
.20944/preprints202310.1698.v1

Figure 4. The Fresnel lens detector structure

Table 1 displays a summary of the weigh
components.

Table 1. Weight estimation of

Components
Detector Structure and La
PMT detector
GBS MCA527OEM + onboa
air-ground communicatio
TOTAL

integrated with the DJI Matrice 600 Pro and ready to

ource purged with N2+NO gas mixture have been used for
detector performed in the Drone Research Laboratory
hows the way the gas was administered to the americium
ows how the count rate increases when the source is purged.

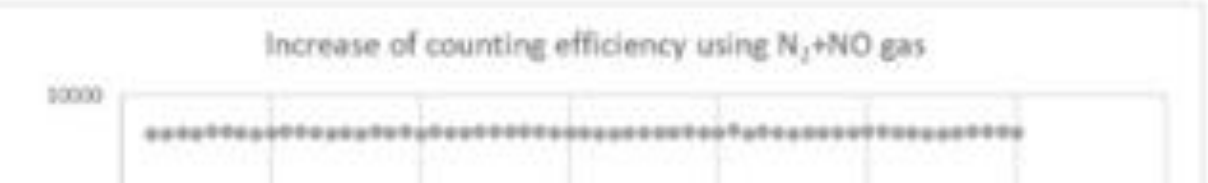

Figure 8. Five UV-C LEDs fabricate

quartz glass dome (#1)

4. Concl

The
detected

MATE's participation in the project

As a consortium partner MATE *with collaboration IDEAS Science Ltd.(managing director Dr. Györgyi Bela)*

- is currently developing on-line curriculum which can be used in BSc and MSc level university education,
- this curriculum can also be integrated into the training system of CBRN specialists, persons responsible for nuclear medicine technologies, radiation safety officers, environmental protection and waste management officers too.
- the topic of the project was simultaneously introduced into the MATE education system, and the educational experiences gained in teaching the related subject will also be taken into account in the development of the above-mentioned on-line course material.

(extracting from slide of 28th WORKSHOP ON ENERGY AND ENVIRONMENT, December 8-9, 2022, Gödöllő, Hungary)

-Partecipation in measuring campaign: Bucharest, IFIN-HH (Horia Hulubei National Institute, Romania, 2023. februar) *with collaboration Crydet Ltd. (managing director Zoltán Csiki)*

- dissemination at leader hungarian institutes: Wigner Research Center for Physics,

MATE
MAGYAR AGRÁR- ÉS ÉLETTUDOMÁNYI EGYETEM

ideas science

High-quality technological solutions and consulting services for environmental and security problems.

CRYDET

Manufacture of scintillation crystals and detectors

wigner

eli attosecond

Educational benefits

MAGYAR AGRÁR- ÉS ÉLETTUDOMÁNYI EGYETEM

Deeper physical foundation on

- alpha radiation (penetration depth in mediums, Bragg-Kleeman –rule, linear energy transfer (LET), the Bragg-curve, computation in Bethe-Bloch formula, measuring methods by conventional detectors: GM-tubes,

- Molecular spectroscopy of diatomic molecules (rotational, vibrational states, infrared spectroscopy, Raman spectroscopy, electronic states associated with angular momentum, indicatings, electronic selection rules, the Franck-Condon principles, quantum mechanical basics, fluorescence and Raman scatterings

- The radioluminescence measuring methods, the so-called First Positive Group of Nitrogen and the Second Negative Group of N2+ ions, optical imaging systems, the lens-PMT, filter-CCD camera systems

Conclusion

MAGYAR AGRÁR- ÉS ÉLETTUDOMÁNYI EGYETEM

The teaching of the subject provides an excellent opportunity to broaden physics education with which the principles of spectroscopy and molecular spectroscopy in particular, as well as the teaching the methods of the fundamentals of quantum mechanics, can become attractive and important for engineering students (extracting from slide of 28th WORKSHOP ON ENERGY AND ENVIRONMENT, December 8-9, 2022, Gödöllő, Hungary)

Thank You for your kind attention!

Need for novel-type detection system for alpha emitters

MAGYAR AGRÁR- ÉS ÉLETTUDOMÁNYI EGYETEM

- Attacks on nuclear power plants
- deployment of the dirty bomb (have a shocking effect on public opinion.)
- previous serious reactor accidents (Chernobyl, Fukushima)

„…Alpha particles represent the biggest risk to soft biological tissues compared to all nuclear decay products due to their high energy, large mass and high linear energy transfer. The amount of deposited energy is about 2 000 000 to 6 000 000 times higher than that of an ordinary chemical reaction (ordinary chemical energy used by the cells in the body), thus implying that a single alpha particle has the ability to severely damage or kill all cells within its range (typically, two to four cells). Therefore, the release of alpha emitting radionuclides in the environment, such as by nuclear terroristic attacks or transportation accidents, as well as by severe emergencies in nuclear installations, represents the greatest radiological threat for human beings if they enter the human body…."

„…Due to the short range of alpha particles, traditional detectors which require direct interaction with the alpha particles must be used in very close proximity to a contaminated surface, around 1 cm…"

Crompton et al (2018), Sensors, 18, 1015; doi:10.3390/s18041015

„…A detection system to measure large-scale contamination of these radionuclides is currently not available…"

(Publishable Summary for 19ENV02 RemoteAlpha)

Challenges and breakthroughs in alpha radiation detection, with a focus on the innovative RemoteAlpha project

I.R. Nikolényi , Z. Gémesi

(1) Institute of Mathematics and Basic Science, (2) Research teacher, MATE
Hungarian University of Agriculture and Life Sciences
Páter K. u. 1., Gödöllő, H-2100 Hungary
E-mail: Nikolenyi.Istvan.Robert@uni-mate.hu

Experimental Learning Day for Students on Radiology

November 27, 2023, Gödöllő, Hungary

HUNGARIAN UNIVERSITY OF AGRICULTURE AND LIFE SCIENCES

mations about Horizon, EMPIR 2020 19ENV02 RemoteAlpha project. Partners

MATE
MAGYAR AGRÁR- ÉS ÉLETTUDOMÁNYI EGYETEM

s://www.euramet.org/researchinnovation/search-research-ects/details/project/remote-and-real-timeoptical-detection-of-alpha-tting-radionuclides-in-the-environment/.

OTHER PARTICIPANTS

Alfa Rift Oy (Finland)
Gottfried Wilhelm Leibniz Universität Hannover (Germany)
Magyar Agrár- és Élettudományi Egyetem (Hungary)
Tampereen korkeakoulusäätiö sr (Finland)
Universitat Politècnica de Catalunya (Spain)

https://remotealpha.drmr.nipne.ro/partners.php

Remote and real-time optical detection of alpha-emitting radionuclides in the environment

Home | Project | Information | Members Area | Blog | Contact | GDPR

PTB
Physikalisch-Technische Bundesanstalt

KORMÁNYHIVATALOK
Budapest Főváros Kormányhivatala

IFIN-HH
"Horia Hulubei" National Institute for R&D in Physics and Nuclear Engineering

Alfa Rift Oy
Alfa Rift Oy

Tampere University
Tampereen korkeakoulusäätiö sr

Leibniz Universität Hannover
Gottfried Wilhelm Leibniz Universität Hannover

UNIVERSITAT POLITÈCNICA DE CATALUNYA BARCELONATECH
Universitat Politècnica de Catalunya

SZENT ISTVÁN UNIVERSITY
Szent István University

MATE
HUNGARIAN UNIVERSITY OF AGRICULTURE AND LIFE SCIENCES

This project 19ENV02 RemoteALPHA has received funding from the EMPIR programme co-financed by the Participating States and from the European Union's Horizon 2020 research and innovation programme.